

Supporting Information

Roles of Niobium on the Dehydrogenation of Propane to Propylene over Pt/Nb-modified Al₂O₃ Catalyst

Tianhao Zhao[Ⓐ], Shanshan Shen[Ⓐ], Yanyan Jia[Ⓑ], Chih-Wen Pao[Ⓒ], Jeng-Lung Chen[Ⓒ], Yong Guo[Ⓐ], Xiaohui Liu[Ⓐ], Sheng Dai^{*Ⓑ}, Yanqin Wang^{*Ⓐ}

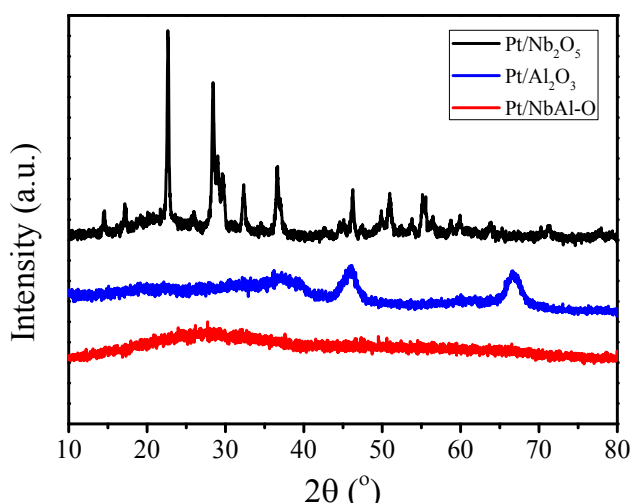


Figure S1. XRD patterns of fresh Pt/Nb₂O₅, Pt/NbAl-O and Pt/Al₂O₃.

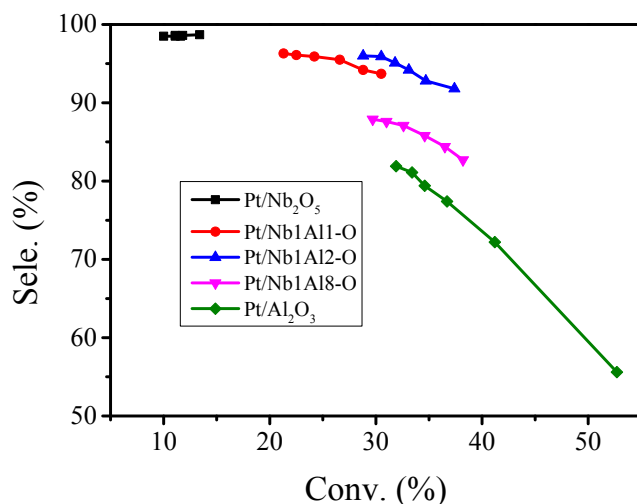


Figure S2. The curve of selectivity vs. conversion rate over different catalysts.

The figure of Selectivity vs. conversion over various catalysts was shown in Figure S2. Although there are differences in the conversion of these catalysts, but the selectivity over

Pt/Nb1Al2-O is always the highest at the same conversion, which means that Pt/Nb1Al2-O has the best performance among these catalysts.

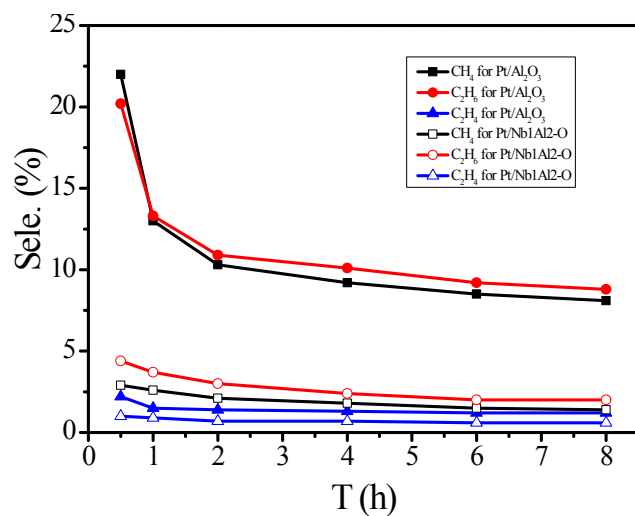


Figure S3. The selectivity of by-products (CH₄, C₂H₆ and C₂H₄) over Pt/Al₂O₃ and Pt/Nb1Al2-O.

Table S1. The deactivation rate parameter of each sample.

| | Pt/Nb ₂ O ₅ | Pt/Nb1Al1-O | Pt/Nb1Al2-O | Pt/Nb1Al8-O | Pt/Al ₂ O ₃ |
|------------|-----------------------------------|-------------|-------------|-------------|-----------------------------------|
| κ_d | 0.0442 | 0.0644 | 0.0520 | 0.0507 | 0.1155 |

Notes: The reaction time is 8 h. The calculation formula is

$$\kappa_d = \frac{\ln \left[\frac{(1 - Conv_{end})}{Conv_{end}} \right] - \ln \left[\frac{(1 - Conv_{start})}{Conv_{start}} \right]}{t}$$

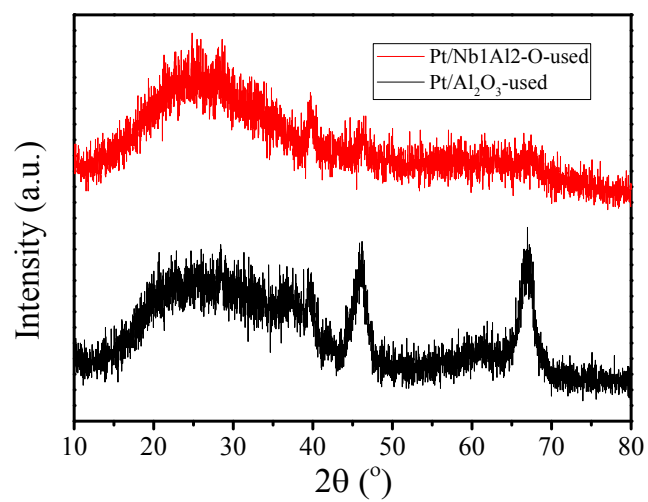


Figure S4. XRD patterns of the used catalysts (Pt/Al₂O₃ and Pt/Nb1Al2-O).

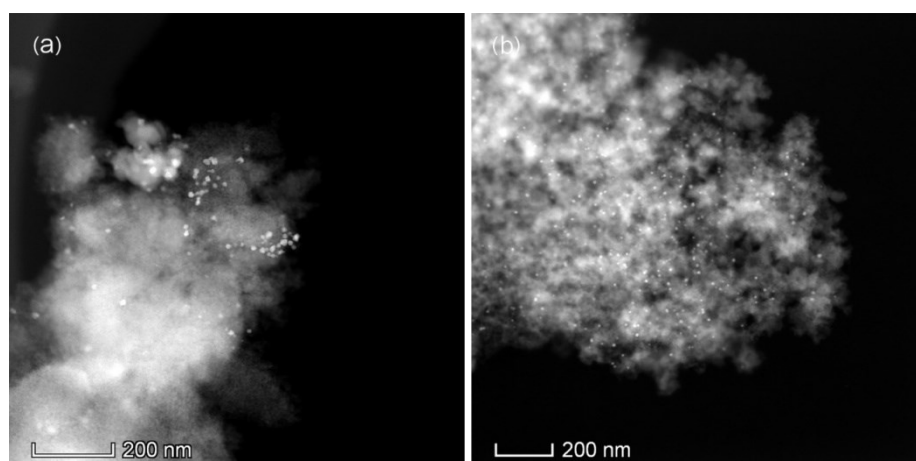


Figure S5. HAADF-STEM images of (a) Pt/Al₂O₃-used, (b) Pt/Nb1Al2-O-used.

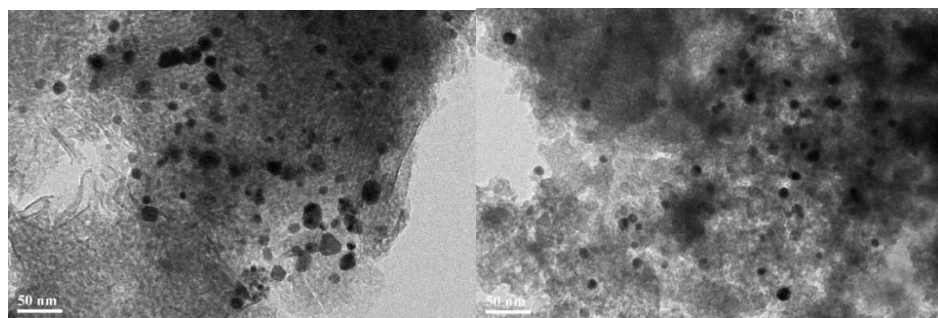


Figure S6. TEM images of Pt/Al₂O₃-used 3 cycles (left) and Pt/Nb1Al2-O-used 3 cycles (right).

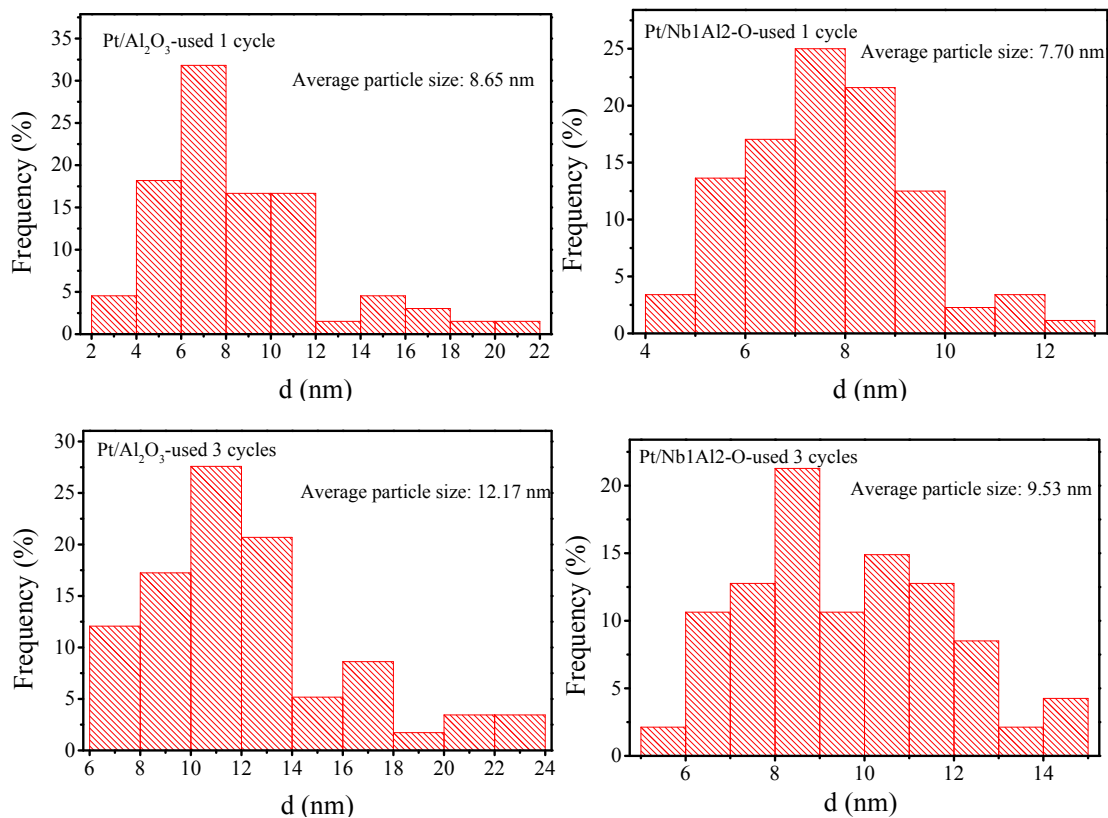


Figure S7. The distribution of Platinum particle size over different used catalysts.

Table S2. The amount of each acid site in Pt/Al₂O₃ and Pt/Nb1Al2-O.

| | NH₃ uptaken (μmol·g⁻¹) | | |
|-----------------------------------|---|-------------|-------------|
| | Weak acid | Medium acid | Strong acid |
| Pt/Al ₂ O ₃ | 166.4 | 95.9 | 264.6 |
| Pt/Nb1Al2-O | 163.0 | 207.9 | 238.9 |

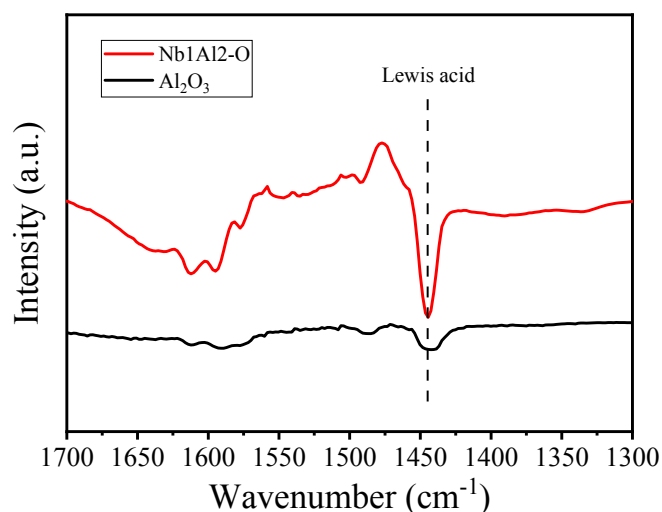


Figure S8. Py-FTIR spectra under vacuum of various catalysts.

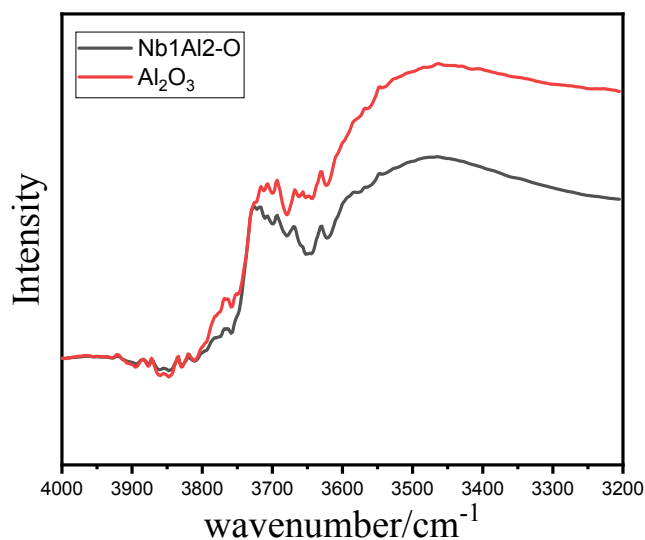


Figure S9. The DRIFTS spectra of both catalysts in 500 °C.

We carried out the Py-FTIR to identify the Lewis and Brønsted acidity under vacuum, the spectra is present in Figure S8. It can be seen that Nb1Al2-O catalyst has markedly higher Lewis acid amount than Al₂O₃, which results in the excellent reaction performance over Pt/Nb1Al2-O. However, the Brønsted acid, located in 1540 cm⁻¹, can hardly be found in all kinds of samples. This inconsistency with NH₃-TPD may come from the larger molecular size of pyridine than ammonium, which cannot reach -OH groups in the pores of samples.

Therefore, additional diffuse reflectance infrared Fourier transform spectroscopy (DRIFTS) was used to compare the numbers of -OH groups on each sample, as it is known that Brønsted acid is always related to -OH groups and it was demonstrated that the peak between 3700 cm⁻¹

and 3680 cm^{-1} is ascribed to surface hydroxyl groups. Before measurement, all samples were pretreated at $500\text{ }^{\circ}\text{C}$ and the DRIFT is shown in Figure S9. It can be seen clearly that the amount of hydroxyl groups on Al_2O_3 is larger than that on Nb1Al2-O , which may be come from the transformation of Al-OH species to Al-O-Nb after introducing Nb into Al_2O_3 and lead to the decrease of Brønsted acid sites in the Nb1Al2-O .

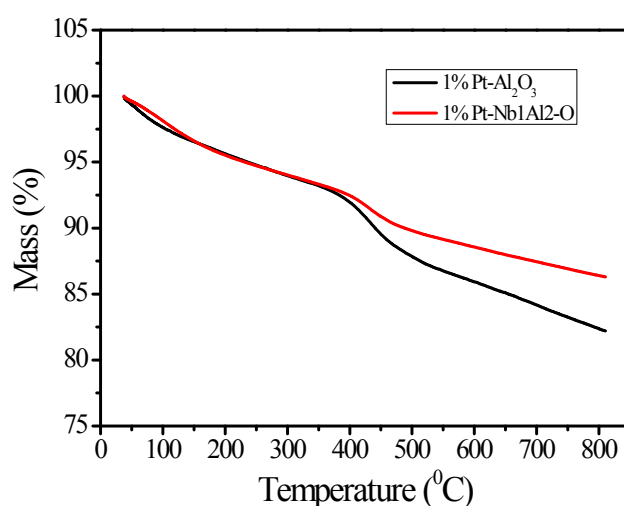


Figure S10. TG curve of the used $\text{Pt}/\text{Al}_2\text{O}_3$ and $\text{Pt}/\text{Nb1Al2-O}$ catalysts.

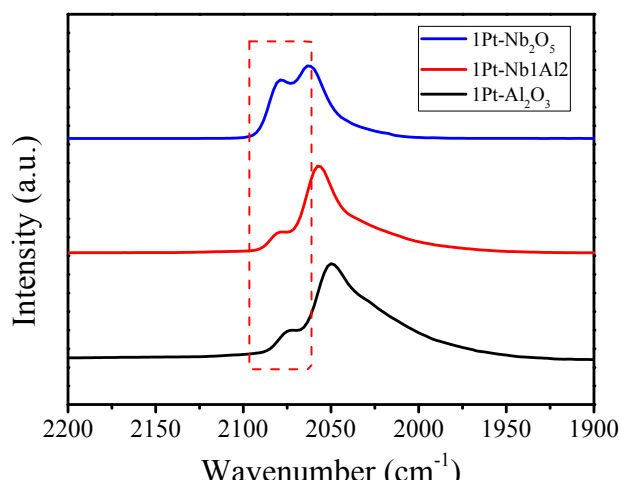


Figure S11. CO-DRIFTS of the $\text{Pt}/\text{Al}_2\text{O}_3$, $\text{Pt}/\text{Nb1Al2-O}$ and $\text{Pt}/\text{Nb2O}_5$.

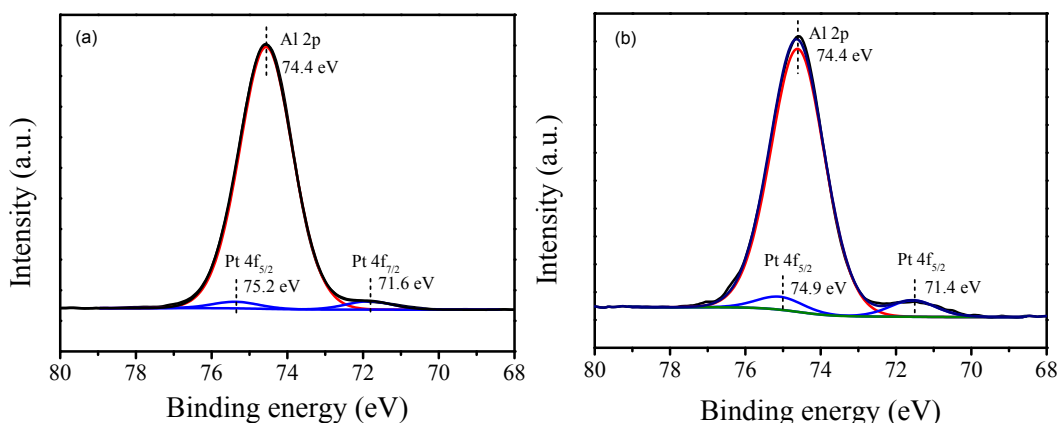


Figure S12. Pt 4f and Al 2p XPS spectra of (a) Pt/Al₂O₃ and (b) Pt/Nb1Al2-O.

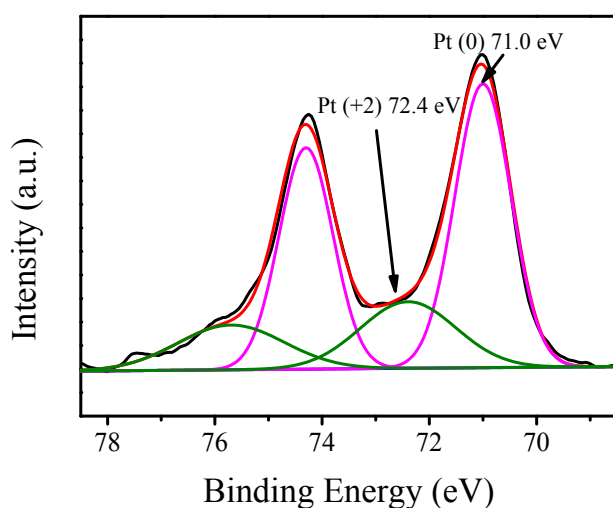


Figure S13. Pt 4f XPS spectra of Pt/Nb₂O₅.

The spectra of Pt 4f and Al 2p over Pt/Al₂O₃ and Pt/Nb1Al2-O catalysts were presented in Figure S12. With careful deconvolution of the overlapped peaks of Al 2p and Pt 4f, it can be seen that the binding energy of Pt is close to that of metallic Pt in both samples. The binding energy of Pt 4f_{7/2} in Pt/Al₂O₃ is 71.6 eV, slightly higher than that of Pt/Nb1Al2-O (71.4 eV), indicating there is less electron on Pt over Pt/Al₂O₃ catalyst. XPS spectra of Pt 4f for Pt/Nb₂O₅ catalyst are shown in Figure S13, and an obvious lower binding energy (71.0 eV) was observed, which means there may be an electron transfer from NbO_x to Pt. Compared with Pt/Al₂O₃, more electrons around Pt over Pt/Nb1Al2-O can decrease the adsorption of propylene and

reduce coke formation.

The XPS spectrum of Pt 4f over Pt/Nb₂O₅ was given in Figure S12. Consistent with our expectations, the binding energy of Pt 4f 7/2 is 71.0 eV, which is the lowest over these three catalysts (Pt/Nb₂O₅, Pt/Nb1Al2-O and Pt/Al₂O₃). However, there are still peaks of Pt (+2) over Pt/Nb₂O₅ catalyst, which may be due to the slight oxidation process.

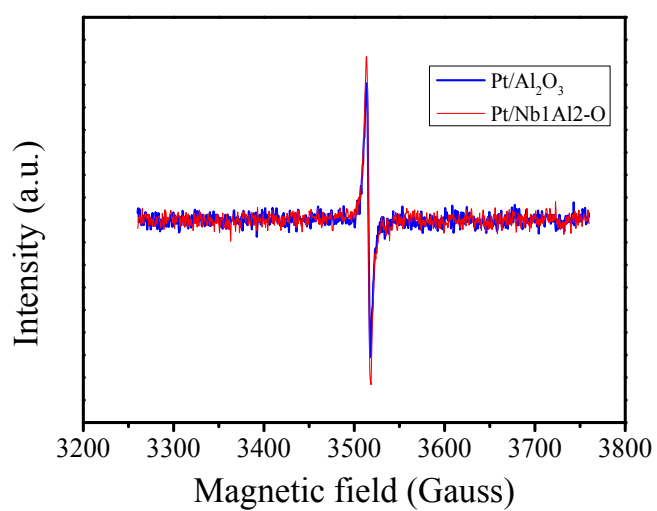


Figure S14. Low temperature EPR spectra of Pt/Al₂O₃ and Pt/Nb1Al2-O catalysts.